The effect of interorbital scattering on superconductivity in doped Dirac materials

David Dentelski,[1,2] Vladyslav Kozii,[3,4] and Jonathan Ruhman[1,2]

[1] *Department of Physics, Bar-Ilan University, 52900, Ramat Gan Israel*
[2] *Center for Quantum Entanglement Science and Technology, Bar-Ilan University, 52900, Ramat Gan Israel*
[3] *Department of Physics, University of California, Berkeley, CA 94720, USA*
[4] *Materials Sciences Division, Lawrence Berkeley National Laboratory, Berkeley, CA 94720, USA*

Unconventional superconductivity has been discovered in a variety of doped quantum materials, including topological insulators, semimetals and twisted bilayers. A unifying property of these systems is strong orbital hybridization, which involves pairing of states with non-trivial Bloch wave functions. In contrast to naive expectation, however, many of these superconductors are relatively resilient to disorder. Here we study the effects of a generic disorder on superconductivity in doped three-dimensional Dirac systems, which serve as a paradigmatic example for the dispersion near a band crossing point in quantum materials. We argue that due to strong orbital hybridization, interorbital scattering processes are naturally present and must be taken into account. We calculate the reduction of the critical temperature for a variety of pairing states and interorbital scattering channels using Abrikosov-Gor'kov theory. In that way, the role of disorder is captured by a single parameter Γ, the pair scattering rate. This procedure is very general and can be readily applied to different band structures and disorder configurations, including magnetic impurities. Our results show that interorbital scattering has a significant effect on superconductivity, where the robustness of different pairing states highly depends on the relative strength of the different interorbital scattering channels. Our analysis also reveals a protection, analogous to the Anderson's theorem, of the odd-parity pairing state with total angular momentum zero (the B-phase of superfluid ^{3}He). This odd-pairty state is a singlet of partners under $\mathcal{CT}$ symmetry (rather than $\mathcal{T}$ symmetry in the standard Anderson's theory), where $\mathcal{C}$ and $\mathcal{T}$ are chiral and time-reversal symmetries, respectively. As a result, it is protected against any disorder potential that respects $\mathcal{CT}$ symmetry, which includes a family of time-reversal odd (magnetic) impurities.

I. INTRODUCTION

Anderson's theory explains why conventional s-wave superconductors are weakly affected by non-magnetic disorder [1–3]. It is based on two essential conditions. The first one is that the Cooper pairs in these superconductors form singlet states of time-reversed partners. The second one is that the phase of the pair wave function is featureless over the entire Fermi surface. These two ensure that the pairing interaction, written in the basis that diagonalizes the disorder potential, remains the same as in the clean limit. Consequently, one can always pair time-reversed partners with the same interaction and the same transition temperature [4]. In contrast, the Cooper pairs in unconventional superconductors violate one of these conditions and, as a result, are not protected [5–22].

From the theoretical perspective, the conditions to prefer pairing in non-s-wave channels are quite stringent, even without the destructive effect of disorder. Nonetheless, a large body of recent experimental measurements, performed in doped topological materials, are consistent with an unconventional superconducting state [23–36], which was predicted theoretically [37–42]. Surprisingly, these superconductors are extremely robust to disorder [43–47].

Mechanisms based on the huge spin-orbit coupling characterizing the topological materials have been suggested to explain this robustness. The authors of Ref. [48] studied the effect of disorder on an odd-parity paring state with zero total angular momentum (equivalent to the B-phase in superfluid ^{3}He). They found that an additional chiral symmetry can protect this state from cer-

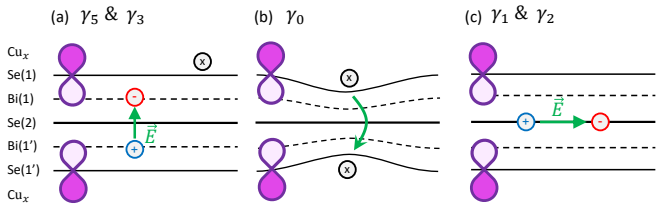

FIG. 1. A schematic picture of different types of non-trivial time-reversal-symmetric intra- and interorbital disorder potentials in Bi_2Se_3. The solid and dashed lines represent the Se and Bi layers in the quintuple unit cell, respectively. The purple p_z orbitals represent the itinerant states on the top and bottom Se layers, which disperse as Dirac fermions close to the Γ-point. (a) Disorder that breaks the symmetry between top and bottom layers induces γ_5 and γ_3 potentials [our convention for the γ matrices is given below Eq.(1)]. This can be caused either by a polar impurity in the z-direction or a charged impurity closer to one layer than the other (e.g., due to the intercalation of Cu). (b) Disorder causing squeezing or stretching of the z-axis lattice constant modifies the hopping between the layers and thus induces a mass term of the form γ_0. (c) An in-plane polar impurity cases, γ_1 and γ_2 potentials. We note that in all cases we also anticipate an intraorbital density potential (proportional to the identity matrix).

tain types disorder when it is present. It was later suggested that the pair wavefunction in doped Bi_2Se_3 is a multi-component nematic state which breaks the rotational symmetry of the crystal [39, 49]. Refs. [46, 50] studied the effect of disorder on the nodal nematic state, also arguing for some robustness, however their results were based on less generic grounds. See also a recent comprehensive study of the effects of scalar disorder on unconventional paring in topological materials [51].

The studies mentioned above, however, focus only on the effects of intraorbital scattering, which has equal weight on all orbitals (i.e., density disorder). Because topological materials are multiorbital systems with huge orbital hybridization, interorbital scattering is not expected to be particularly weaker than density disorder. In Fig. 1 we schematically depict three types of time-reversal-symmetric disorder potentials, which are expected to be present in Bi_2Se_3 and lead to interorbital scattering. Thus, it is important to understand the effects of interorbital scattering in the superconducting topological materials.

The influence of interorbital scattering on pairing was first emphasized by Golubov and Mazin [52] and was later studied in the context of systems with multiple Fermi surfaces (see, for example, Ref. [53–57]). We emphasize that in topological materials the multiorbital nature is embedded in the Bloch wave-functions rather than the presence of multiple Fermi surfaces, making them somewhat different.

In this paper, we study the effect of short-ranged intra- and interorbital scattering on superconductivity in three-dimensional materials with massless Dirac dispersion. Namely, we provide an extensive picture of how the transition temperature T_c in different pairing channels is affected by all possible types of short-ranged scattering potentials. The Dirac dispersion is a paradigmatic example of dispersion in topological materials, which naturally have large spin-orbit coupling [58].

Our results are expressed in terms of the pair-breaking rate Γ, which also enters the Abrikosov-Gor'kov theory of superconductors with magnetic impurities [2]; they are summarized in Table II. We find that the only state robust to time-reversal symmetric (TRS) disorder is the s-wave, in agreement with the Anderson's theorem [1]. Another fully gapped isotropic state is the odd-parity state with zero total angular momentum (analogous to the B-phase in superfluid ^{3}He), which does not exhibit such robustness, in contrast to previous expectations [47, 48]. Despite being protected against certain types of disorder, it turns out to be very sensitive to some other types of defects, such as mass and polar impurities, which we expect to be generally present in topological materials.

On the other hand, we find that this fully isotropic odd-parity state is protected from any disorder that respects $\mathcal{CT}$ (assuming this symmetry is also present in the clean system), where $\mathcal{C}$ and $\mathcal{T}$ are chiral and time-reversal symmetries, respectively. The reason for such robustness is that this state corresponds to a singlet pairing state of $\mathcal{CT}$ partners, in perfect analogy to pairing of $\mathcal{T}$-partners in Anderson's original argument [1]. Interestingly, this result implies that this fully gapped odd-parity state is protected against certain disorder potentials that are odd under time-reversal $\mathcal{T}$.

We also study the multicomponent states, which are the $O(3)$-symmetry group analogs the nematic pairing states in doped Bi_2Se_3. These states evolve into each other when the symmetry group is reduced from the fully isotropic $O(3)$ to trigonal D_{3d} group of Bi_2Se_3. We find that these multicomponent pairing states can be more robust than the corresponding states in systems without spin-orbit coupling. However, they are still more susceptible to disorder than what was previously suggested [46, 50]. In addition, we consider the effect of magnetic impurities and find that the multicomponent states are also relatively robust (not completely though). In particular, we find that these states are less susceptible to magnetic disorder than the s-wave state. Thus, nematic superconducting state can possibly be stabilized by magnetic impurities. It should be added that when time-reversal is broken the chiral state might be preferred over the nematic one [59–62].

We emphasize that in this paper we consider the specific case of a massless Dirac systems at finite doping, though it can be easily generalized to the finite mass case and other topological dispersion relations, including semimetals with the quadratic band touching points, line-node semimetals and three band touching points.

The rest of this paper is organized as follows. In Sec. II we present the basic ingredients of our model, namely, an action for a massless Dirac fermion subjected to a generic disorder potential and an attractive pairing interaction. We project the disorder onto the Bloch basis of the conduction electrons near Fermi surface, which we will use throughout this paper. In Sec. III we calculate the pair breaking rate Γ in topological materials, which is the main parameter that affects T_c and the whole thermodynamics. Our results are presented in Sec. IV, where we discuss the effect of different types of disorder on the various pairing channels. Finally, Sec. V provides a summary of our main results and a discussion of the application of our method for other systems. Multiple technical details of our calculation are delegated to Appendices.

II. THE MODEL

We start by describing the normal-state action of the model. We consider massless Dirac fermions

$$\mathcal{S}_0 = \sum_{\omega,\boldsymbol{k}} \psi^\dagger_{\omega,\boldsymbol{k}} \left[-i\omega + iv\boldsymbol{k}\cdot\gamma_0\boldsymbol{\gamma} - \epsilon_F\right]\psi_{\omega,\boldsymbol{k}}, \qquad (1)$$

where $\psi^\dagger_{\omega,\boldsymbol{k}} = \left(\psi^\dagger_{\omega,\boldsymbol{k},+} \;\; \psi^\dagger_{\omega,\boldsymbol{k},-}\right)$, $\psi_{\omega,\boldsymbol{k},\pm}$ correspond to two orbitals, each consisting of a Kramers pair. The orbitals are related to each other through inversion. v is an isotropic velocity and ϵ_F is the Fermi energy. In addition, the γ matrices are taken to be Hermitian, $\boldsymbol{\gamma} = \tau_2\boldsymbol{s}$,

$\gamma_0 = \tau_1 s_0$ and $\gamma_5 = \gamma_0\gamma_1\gamma_2\gamma_3 = -\tau_3 s_0$, where $\boldsymbol{\tau}$ and $\boldsymbol{s}$ are Pauli matrices in the orbital and spin basis, correspondingly. Note that we neglect the mass term and any higher order corrections in momentum.

The action in Eq. (1) can be conveniently diagonalized in the manifestly covariant Bloch basis (MCBB), in which the electron spinor transforms as an ordinary $SU(2)$ spin-1/2 [40, 49, 63, 64]: $|\hat{\boldsymbol{k}}, 1, \zeta\rangle = \frac{1}{2}\left(\zeta - \hat{k}_z,\ -\hat{k}_+,\ \zeta + \hat{k}_z,\ \hat{k}_+\right)^T$ and $|\hat{\boldsymbol{k}}, 2, \zeta\rangle = \frac{1}{2}\left(-\hat{k}_-,\ \zeta + \hat{k}_z,\ \hat{k}_-,\ \zeta - \hat{k}_z\right)^T$, where $\zeta = \pm 1$ corresponds to conduction/valence band, respectively, $\hat{k}_j = k_j/k$, and $\hat{k}_\pm = \hat{k}_x \pm i\hat{k}_y$. Without loss of generality we assume electron doping ($\zeta = 1$), and therefore omit index ζ henceforth. The field operators are then approximated by their weight on the band operators $\psi_k \approx |\hat{\boldsymbol{k}}, 1\rangle c_{\boldsymbol{k},1} + |\hat{\boldsymbol{k}}, 2\rangle c_{\boldsymbol{k},2}$.

Finally, the action in Eq. (1) possesses inversion, chiral, and time-reversal symmetries. The representation of these symmetry operations in orbital basis is given by $\mathcal{I} = \gamma_0$, $\mathcal{C} = \gamma_5$, and $\mathcal{T} = \mathcal{K}\gamma_1\gamma_3$, respectively, where $\mathcal{K}$ is complex conjugation.

Next, we consider the disorder potential. The crucial element in our theory is the inclusion of interorbital scattering. Within the Dirac notations, such (momentum-independent) scatterings can be represented using the Dirac matrices introduced above and their products. For elastic short-ranged scattering (compared to k_F) we have

$$\mathcal{S}_d = \sum_{m=0}^{15}\sum_{l=1}^{N_m}\sum_{\omega,\boldsymbol{k},\boldsymbol{p}} V_{l,m}\, e^{i(\boldsymbol{k}-\boldsymbol{p})\cdot\boldsymbol{r}_l}\psi^\dagger_{\omega,\boldsymbol{p}} M_m \psi_{\omega,\boldsymbol{k}}, \qquad (2)$$

where N_m is the number of impurities in channel m and $\boldsymbol{r}_l$ is the positions of these short-ranged impurities. There are 16 different Hermitian matrices M_m representing different types of disorder. The representation of these matrices in the orbital-spin $\tau \otimes s$ basis and their discrete symmetry properties are given in Table I. We further clarify that $m = 0$ corresponds to simple density disorder $\mathbb{1}$, which was considered in Refs. [46, 48, 50, 51]. $m = 1$ corresponds to mass disorder γ_0, $m = 2$ is odd-parity scalar disorder γ_5, $m = 3, 4, 5$ correspond to odd-parity dipolar disorder and the magnetic disorder $m = 6, 7, 8$ correspond to a fully symmetric local moment with spin oriented along the axis $S_\alpha = -i\varepsilon_{\alpha\beta\gamma}\gamma_\beta\gamma_\gamma$. Some examples of non-trivial scattering matrices of this type, which naturally appear in disordered Bi_2Se_3, are shown schematically in Fig. 1. When projecting the disorder potential onto the MCBB, we obtain a set scattering matrices $Q_m(\hat{\boldsymbol{p}}, \hat{\boldsymbol{k}})$ with non-trivial momentum dependence:

$$\mathcal{S}_d = \sum_{m=0}^{15}\sum_{l=1}^{N_m}\sum_{\omega,\boldsymbol{k},\boldsymbol{p}} V_{l,m}\, e^{i(\boldsymbol{k}-\boldsymbol{k}')\cdot\boldsymbol{r}_l} c^\dagger_{\omega,\boldsymbol{p}} Q_m(\hat{\boldsymbol{p}}, \hat{\boldsymbol{k}}) c_{\omega,\boldsymbol{k}}, \quad (3)$$

where $c^\dagger_{\omega,\boldsymbol{p}} = (c^\dagger_{\omega,\boldsymbol{p},1}, c^\dagger_{\omega,\boldsymbol{p},2})$, and we defined the matrices $Q^{\alpha\beta}_m(\hat{\boldsymbol{p}}, \hat{\boldsymbol{k}}) \equiv \langle \hat{\boldsymbol{p}}\alpha | M_m | \hat{\boldsymbol{k}}\beta\rangle$, which are listed in Table I.

Before proceeding, we make a few important remarks regarding the choice of disorder potential in Eq. (2). First, we assume that the disorder is Gaussian correlated with zero mean, $\langle V_{l,m}\rangle = 0$. Next, we assume that there is no spatial correlations, and that different types of disorder do not correlate. The latter assumption implies that disorder potential does not break any symmetry *on average*, leading to $\langle V_{l,m} V_{l',m'}\rangle = V_m^2 \delta_{mm'}\delta_{ll'}$. There is one exception, however, which requires clarification. In the absence of chiral symmetry, the density disorder ($m = 0$) and the mass disorder ($m = 1$) can, in principle, mix, since they belong to the same trivial representation. We note that this is the reason why mass disorder is always present in Bi_2Se_3, even if it respects time-reversal and inversion symmetries (as opposed to the claim made in Ref. [46]). As we show in Sec. III, however, the correlations between $m = 0$ and $m = 1$ disorder channels do not affect the scattering rate or superconductivity.

Second, a central assumption of our theory is that disorder naturally appears in the *orbital basis*. Indeed, the set of matrices $Q_m(\hat{\boldsymbol{p}}, \hat{\boldsymbol{k}})$ introduced in Eq. (3) and listed in Table I is the result of starting from the orbital basis and projecting disorder potential onto the MCBB on the Fermi surface. The additional momentum-dependent form-factors in the scattering matrices could have been easily overlooked if we started directly from the band basis, constructing a phenomenological picture of disorder [65]. To emphasize this fact, we point out that even the density channel obtains non-trivial momentum dependence, which, as we show below, plays a crucial role in protecting some unconventional pairing states from density disorder.

The last ingredient required to estimate the superconducting transition temperature is the attractive interaction which leads to the instability. We study the superconducting instability in the *band basis*, in the spirit of the Bardeen-Cooper-Schrieffer (BCS) theory. We then decompose the interaction into the irreducible representations in the Cooper channel:

$$\mathcal{S}_I = -\frac{1}{2}\sum_{\boldsymbol{k},\boldsymbol{p},J} g_J \left[c^\dagger_{\boldsymbol{p}} F^\dagger_J(\hat{\boldsymbol{p}}) c^\dagger_{-\boldsymbol{p}}\right]\left[c_{-\boldsymbol{k}} F_J(\hat{\boldsymbol{k}}) c_{\boldsymbol{k}}\right], \qquad (4)$$

where $F_J(\hat{\boldsymbol{k}})$ are form-factors in the MCBB corresponding to different representations J of the relevant symmetry group (see Appendix B). A superconducting instability can occur in any one of the channels depending on the attractive strength of coefficients g_J. We are mainly interested in systems with large spin-orbit coupling, characteristic for topological materials, which do not have spin-rotational symmetry. Instead, in this paper we focus on the fully isotropic $O(3)$ group of *joint* rotations of spin and momentum. Different representations are labeled by the total angular momentum J, and the corresponding form-factors are listed in Table III. (Note that within our notations J labels both different representations and different components within the same representation.)

m	$\mathcal{I}$	$\mathcal{T}$	$\mathcal{C}$	Orbital Matrix - M_m	Band Matrix - $\langle\hat{\boldsymbol{p}}\zeta\|M_m\|\hat{\boldsymbol{k}}\zeta\rangle$
0	+	+	+	$\mathbb{1} = \tau_0 s_0$	$Q_0(\hat{\boldsymbol{p}},\hat{\boldsymbol{k}}) = \frac{1}{2}\left(1+\hat{\boldsymbol{p}}\cdot\hat{\boldsymbol{k}}+i[\hat{\boldsymbol{p}}\times\hat{\boldsymbol{k}}]\cdot\boldsymbol{\sigma}\right)$
1	+	+	-	$\gamma_0 = \tau_1 s_0$	$Q_1(\hat{\boldsymbol{p}},\hat{\boldsymbol{k}}) = \frac{1}{2}\left(1-\hat{\boldsymbol{p}}\cdot\hat{\boldsymbol{k}}-i[\hat{\boldsymbol{p}}\times\hat{\boldsymbol{k}}]\cdot\boldsymbol{\sigma}\right)$
2	-	+	+	$\gamma_5 = -\tau_3 s_0$	$Q_2(\hat{\boldsymbol{p}},\hat{\boldsymbol{k}}) = \frac{\zeta}{2}\left(\hat{\boldsymbol{p}}+\hat{\boldsymbol{k}}\right)\cdot\boldsymbol{\sigma}$
3	-	+	-	$\gamma_1 = \tau_2 s_1$	$Q_3(\hat{\boldsymbol{p}},\hat{\boldsymbol{k}}) = \frac{\zeta}{2}\left\{i\left(\hat{\boldsymbol{p}}-\hat{\boldsymbol{k}}\right)_x+[(\hat{\boldsymbol{p}}+\hat{\boldsymbol{k}})\times\boldsymbol{\sigma}]_x\right\}$
4	-	+	-	$\gamma_2 = \tau_2 s_2$	$Q_4(\hat{\boldsymbol{p}},\hat{\boldsymbol{k}}) = \frac{\zeta}{2}\left\{i\left(\hat{\boldsymbol{p}}-\hat{\boldsymbol{k}}\right)_y+[(\hat{\boldsymbol{p}}+\hat{\boldsymbol{k}})\times\boldsymbol{\sigma}]_y\right\}$
5	-	+	-	$\gamma_3 = \tau_2 s_3$	$Q_5(\hat{\boldsymbol{p}},\hat{\boldsymbol{k}}) = \frac{\zeta}{2}\left\{i\left(\hat{\boldsymbol{p}}-\hat{\boldsymbol{k}}\right)_z+[(\hat{\boldsymbol{p}}+\hat{\boldsymbol{k}})\times\boldsymbol{\sigma}]_z\right\}$
6	+	-	+	$i\gamma_3\gamma_2 = \tau_0 s_1$	$Q_6(\hat{\boldsymbol{p}},\hat{\boldsymbol{k}}) = \frac{1}{2}\left\{-i[\hat{\boldsymbol{p}}\times\hat{\boldsymbol{k}}]_x+[1-\hat{\boldsymbol{p}}\cdot\hat{\boldsymbol{k}}]\sigma_x+[\hat{p}_x\hat{\boldsymbol{k}}+\hat{\boldsymbol{p}}\hat{k}_x]\cdot\boldsymbol{\sigma}\right\}$
7	+	-	+	$i\gamma_1\gamma_3 = \tau_0 s_2$	$Q_7(\hat{\boldsymbol{p}},\hat{\boldsymbol{k}}) = \frac{1}{2}\left\{-i[\hat{\boldsymbol{p}}\times\hat{\boldsymbol{k}}]_y+[1-\hat{\boldsymbol{p}}\cdot\hat{\boldsymbol{k}}]\sigma_y+[\hat{p}_y\hat{\boldsymbol{k}}+\hat{\boldsymbol{p}}\hat{k}_y]\cdot\boldsymbol{\sigma}\right\}$
8	+	-	+	$i\gamma_2\gamma_1 = \tau_0 s_3$	$Q_6(\hat{\boldsymbol{p}},\hat{\boldsymbol{k}}) = \frac{1}{2}\left\{-i[\hat{\boldsymbol{p}}\times\hat{\boldsymbol{k}}]_z+[1-\hat{\boldsymbol{p}}\cdot\hat{\boldsymbol{k}}]\sigma_z+[\hat{p}_z\hat{\boldsymbol{k}}+\hat{\boldsymbol{p}}\hat{k}_z]\cdot\boldsymbol{\sigma}\right\}$
9	-	-	+	$i\gamma_0\gamma_1 = -\tau_3 s_1$	$Q_9(\hat{\boldsymbol{p}},\hat{\boldsymbol{k}}) = \frac{\zeta}{2}\left\{(\hat{\boldsymbol{p}}+\hat{\boldsymbol{k}})_x-i[(\hat{\boldsymbol{p}}-\hat{\boldsymbol{k}})\times\boldsymbol{\sigma}]_x\right\}$
10	-	-	+	$i\gamma_0\gamma_2 = -\tau_3 s_2$	$Q_{10}(\hat{\boldsymbol{p}},\hat{\boldsymbol{k}}) = \frac{\zeta}{2}\left\{(\hat{\boldsymbol{p}}+\hat{\boldsymbol{k}})_y-i[(\hat{\boldsymbol{p}}-\hat{\boldsymbol{k}})\times\boldsymbol{\sigma}]_y\right\}$
11	-	-	+	$i\gamma_0\gamma_3 = -\tau_3 s_3$	$Q_{11}(\hat{\boldsymbol{p}},\hat{\boldsymbol{k}}) = \frac{\zeta}{2}\left\{(\hat{\boldsymbol{p}}+\hat{\boldsymbol{k}})_z-i[(\hat{\boldsymbol{p}}-\hat{\boldsymbol{k}})\times\boldsymbol{\sigma}]_z\right\}$
12	-	-	-	$i\gamma_0\gamma_5 = -\tau_2 s_0$	$Q_{12}(\hat{\boldsymbol{p}},\hat{\boldsymbol{k}}) = -i\frac{\zeta}{2}\left(\hat{\boldsymbol{p}}-\hat{\boldsymbol{k}}\right)\cdot\boldsymbol{\sigma}$
13	+	-	-	$i\gamma_1\gamma_5 = \tau_1 s_1$	$Q_{13}(\hat{\boldsymbol{p}},\hat{\boldsymbol{k}}) = \frac{1}{2}\left\{i(\hat{\boldsymbol{p}}\times\hat{\boldsymbol{k}})_x-(\hat{p}_x\hat{\boldsymbol{k}}+\hat{k}_x\hat{\boldsymbol{p}})\cdot\boldsymbol{\sigma}+(1+\hat{\boldsymbol{p}}\cdot\hat{\boldsymbol{k}})\sigma_x\right\}$
14	+	-	-	$i\gamma_2\gamma_5 = \tau_1 s_2$	$Q_{14}(\hat{\boldsymbol{p}},\hat{\boldsymbol{k}}) = \frac{1}{2}\left\{i(\hat{\boldsymbol{p}}\times\hat{\boldsymbol{k}})_y-(\hat{p}_y\hat{\boldsymbol{k}}+\hat{k}_y\hat{\boldsymbol{p}})\cdot\boldsymbol{\sigma}+(1+\hat{\boldsymbol{p}}\cdot\hat{\boldsymbol{k}})\sigma_y\right\}$
15	+	-	-	$i\gamma_3\gamma_5 = \tau_1 s_3$	$Q_{15}(\hat{\boldsymbol{p}},\hat{\boldsymbol{k}}) = \frac{1}{2}\left\{i(\hat{\boldsymbol{p}}\times\hat{\boldsymbol{k}})_z-(\hat{p}_z\hat{\boldsymbol{k}}+\hat{k}_z\hat{\boldsymbol{p}})\cdot\boldsymbol{\sigma}+(1+\hat{\boldsymbol{p}}\cdot\hat{\boldsymbol{k}})\sigma_z\right\}$

TABLE I. Table of the impurity scattering matrices in the orbital and band bases appearing in Eqs. (2) and (3). The table also lists the discrete symmetry properties of each scattering process under $\mathcal{I} = \gamma_0 = \tau_1 s_0$, $\mathcal{T} = \mathcal{K}\gamma_1\gamma_3 = \mathcal{K}\tau_0(-is_y)$, and $\mathcal{C} = \gamma_5 = -\tau_3 s_0$, corresponding to inversion, time-reversal and chiral symmetries, respectively.

III. COMPUTATION OF THE SCATTERING RATE

We now turn to the computation of the pair scattering rate Γ, which enters the Abrikosov-Gor'kov theory and dictates the thermodynamics of superconductors. The procedure we employ consists of three main steps, which are described diagrammatically in Fig. 2.

Single-particle lifetime – We start with computing the single-particle lifetime. The bare electronic Green's function in the *band basis* is given by ($\zeta = 1$)

$$G_0(i\omega,\boldsymbol{k}) = \frac{1}{i\omega - vk + \epsilon_F}. \tag{5}$$

Summation of the diagrams in Fig. 2 (a) leads to a self-energy correction to the Green's function, $G^{-1}(i\omega,\boldsymbol{k}) = G_0^{-1}(i\omega,\boldsymbol{k}) - \Sigma(i\omega)$. Using Eqs. (3) and (5), we find that the self-energy is given by $\Sigma(i\omega) = \sum_m \Sigma_m(i\omega)$, with

$$\begin{aligned}\Sigma_m(i\omega) &= \frac{n_m V_m^2}{8\pi^3}\int d^3p\, Q_m(\hat{\boldsymbol{k}},\hat{\boldsymbol{p}})G_0(i\omega,\boldsymbol{p})Q_m(\hat{\boldsymbol{p}},\hat{\boldsymbol{k}}) \\ &= \frac{n_m V_m^2 k_F^2}{4\pi^2}\int_{-\infty}^{\infty}\frac{dp}{i\omega - vp} = -\frac{i\,\mathrm{sign}\,(\omega)}{2\tau_m},\end{aligned} \tag{6}$$

where

$$\tau_m \equiv \frac{1}{\pi\nu_0 n_m V_m^2}. \tag{7}$$

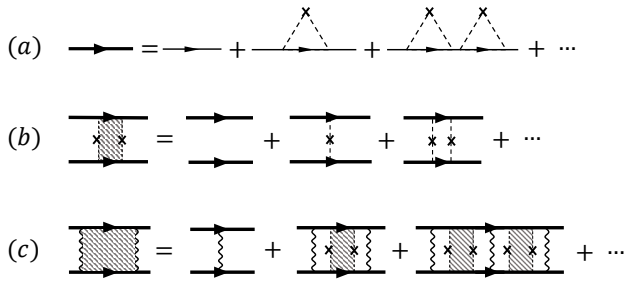

FIG. 2. A diagrammatic representation of the summation of the Gor'kov ladder. (a) The summation over the scattering processes from all types of impurities within the first Born approximation, which leads to the self-energy correction to the full Green's function, Eq. (6). (b) The Cooperon vertex correction $\mathcal{B}_J(i\omega)$, Eq. (12), which results from the summation over the bare pairing propagators $A(i\omega)$, Eq. (9). (c) The summation of the Gor'kov ladder. The building block of the ladder, $\mathcal{P}_J$, is given by the sum of $\mathcal{B}_J(i\omega)$ over Matsubara frequencies, see Eq. (14).

Here $n_m = N_m/L^3$ is the density of impurities in channel m, which arises after averaging over the positions of the impurities, and $\nu_0 = k_F^2/2\pi^2 v$ is the density of

states at the Fermi level per pseudospin. We note a factor of 2 difference in the definition of the scattering time compared to a parabolic band (see Appendix A), which is a feature of topological touching points of two bands. Thus, we have obtained that the single-particle scattering rate decomposes into a sum over the different scattering channels:

$$\frac{1}{\tau} \equiv \sum_m \frac{1}{\tau_m}. \tag{8}$$

We remind that disorder is uncorrelated among different channels, which results from the assumption that disorder does not break any symmetry on average. Mass and density disorder are an exception, since they both belong to the trivial representation. However, we note that even if cross correlations between mass and density impurities are present, they vanish after angle integration over $\hat{\boldsymbol{p}}$ in Eq. (6), making Eq. (8) a generic result within the leading Born approximation.

Vertex correction – In addition to the single-particle processes, it is also important to take into account the effect of pair scattering. Namely, now we calculate the correction to the BCS vertex due to intermediate scattering on disorder. In the limit of weak disorder, $\epsilon_F \tau \gg 1$, the most important correction to the Gor'kov ladder comes from the diagrams with non-intersecting impurity lines (so-called Cooperon), as shown in Fig. 2 (b) [3].

To compute the disorder contribution to the vertex we need two ingredients. First, we calculate the bare propagator of a Cooper pair:

$$A(i\omega) = \sum_{\boldsymbol{p}} \mathrm{Tr}\left[G(i\omega,\boldsymbol{p})F_J^\dagger(\hat{\boldsymbol{p}})G^{\mathrm{T}}(-i\omega,-\boldsymbol{p})F_J(\hat{\boldsymbol{p}})\right] = \frac{k_F^2}{2\pi^2}\int_{-\infty}^{\infty}\frac{dp}{\left(\omega+\mathrm{sign}\,(\omega)/2\tau\right)^2+v^2p^2} = \frac{2\pi\tau\nu_0}{1+2\tau|\omega|}. \tag{9}$$

This propagator links between the scattering events on the Gor'kov ladder and corresponds diagrammatically to the first term on the r.h.s. of Fig. 2 (b) [i.e., it forms the legs of the ladder]. When decomposing a generic pairing interaction into the irreducible representations [as in Eq. (4)], the Gor'kov ladder decomposes into scattering channels of the orthogonal basis functions $F_J(\hat{\boldsymbol{k}})$, which are labeled by J. Thus, when writing Eq. (9), we assume that the Cooper pair propagator is contracted on both sides with the interaction lines in the corresponding channel J.

The next important ingredient for calculating the Gor'kov ladder is the scattering amplitude from a single impurity in particle-particle basis, which the building element of a Cooperon and shown diagrammatically as the second term on the r.h.s. of Fig. 2 (b). Thus, we need the scattering amplitude of a Cooper pair with *any* momenta $\boldsymbol{k}$ and $-\boldsymbol{k}$ into a pair with any other momenta $\boldsymbol{p}$ and $-\boldsymbol{p}$ due to an impurity of type m. This amplitude

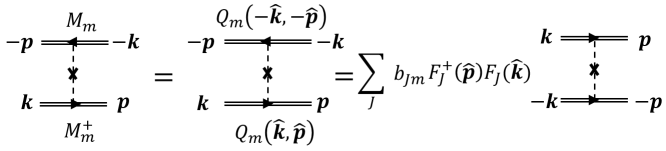

FIG. 3. A diagrammatic representation of the decomposition from particle-hole to particle-particle channels, see Eq. (10). Matrices M, Q, F, and b are defined in Eqs. (2), (3), (4), and (11) [see also Tables I, III, and Eq. (B1)].

is given by the product of two single-particle events:

$$n_m V_m^2 Q_m^{\alpha\beta}(\hat{\boldsymbol{p}},\hat{\boldsymbol{k}})Q_m^{\gamma\delta}(-\hat{\boldsymbol{p}},-\hat{\boldsymbol{k}})c^\dagger_{\boldsymbol{p}\alpha}c_{\boldsymbol{k}\beta}c^\dagger_{-\boldsymbol{p}\gamma}c_{-\boldsymbol{k}\delta} = \frac{1}{\pi\nu_0}\sum_J \frac{b_{Jm}}{\tau_m}c^\dagger_{\boldsymbol{p}}F_J^\dagger(\hat{\boldsymbol{p}})c^\dagger_{-\boldsymbol{p}}\,c_{-\boldsymbol{k}}F_J(\hat{\boldsymbol{k}})c_{\boldsymbol{k}}, \tag{10}$$

where

$$b_{Jm} = \int \frac{d\Omega_{\boldsymbol{k}}d\Omega_{\boldsymbol{p}}}{(4\pi)^2}\mathrm{Tr}\left[Q_m(\hat{\boldsymbol{p}},\hat{\boldsymbol{k}})F_J^\dagger(\hat{\boldsymbol{k}})Q_m^{\mathrm{T}}(-\hat{\boldsymbol{p}},-\hat{\boldsymbol{k}})F_J(\hat{\boldsymbol{p}})\right] \tag{11}$$

is a matrix of weights corresponding to the conversion from the particle-hole to particle-particle basis (similar to the Fierz identity [42]) and $d\Omega_{\boldsymbol{k}} = d(\cos\theta_{\boldsymbol{k}})d\phi_{\boldsymbol{k}}$ is the solid angle element. The matrix in Eq. (11) is given explicitly in Appendix B, here we only note that $|b_{Jm}| \leq 1/2$. The procedure of decomposition from particle-hole to particle-particle basis is shown schematically in Fig. 3.

Contracting the two ingredients, Eq. (9) and Eq. (10), and using the orthogonality of the superconducting form-factors $F_J(\hat{\boldsymbol{k}})$, we obtain for the disorder corrected block of the Gor'kov ladder, shown schematically in Fig. 2 (b):

$$\mathcal{B}_J(i\omega) = \frac{A(i\omega)}{1-A(i\omega)\sum_m b_{Jm}/\pi\nu_0\tau_m} = \frac{\pi\nu_0}{\Gamma_J/2+|\omega|}, \tag{12}$$

where

$$\Gamma_J = \sum_m \Gamma_{Jm} \;\;;\;\; \Gamma_{Jm} \equiv \frac{1-2b_{Jm}}{\tau_m} \tag{13}$$

is the pair scattering rate, which is a sum of independent scattering rates Γ_{Jm} originating from the different intra- and interorbital disorder channels m. The values for the partial pair scattering rates from Eq. (13) are the main result of this paper and are listed in Table II.

Computation of T_c – The final step of the calculation is to use the disorder-modified interaction in the superconducting channel J to compute the renormalized pairing vertex. To do that, we insert a Cooperon in each block of the Gor'kov ladder [this step give us factor $\mathcal{B}_J(i\omega)$], perform the summation over intermediate Matsubara frequencies $\omega_n = \pi T(2n+1)$, and sum up all the blocks [as shown in Fig. 2 (c)]. The result reads as

				$\mathbb{1}$	γ_0	γ_5	γ_1	γ_2	γ_3	$i\gamma_3\gamma_2$	$i\gamma_1\gamma_3$	$i\gamma_2\gamma_1$	$i\gamma_0\gamma_1$	$i\gamma_0\gamma_2$	$i\gamma_0\gamma_3$	$i\gamma_0\gamma_5$	$i\gamma_1\gamma_5$	$i\gamma_2\gamma_5$	$i\gamma_3\gamma_5$
			m	0	1	2	3	4	5	6	7	8	9	10	11	12	13	14	15
			$\mathcal{T}$	+	+	+	+	+	+	-	-	-	-	-	-	-	-	-	-
			$\mathcal{I}$	+	+	-	-	-	-	+	+	+	-	-	-	-	+	+	+
			$\mathcal{C}$	+	-	+	-	-	-	+	+	+	+	+	+	-	-	-	-
L	S	J																	
0	0	$0g$	F_{0g}	0	0	0	0	0	0	2	2	2	2	2	2	2	2	2	2
1	1	$0u$	F_{0u}	0	2	0	2	2	2	2	2	2	2	2	2	0	0	0	0
1	1	11	F_{11}	1/3	5/3	5/3	1/3	5/3	5/3	5/3	1/3	1/3	1/3	5/3	5/3	5/3	1/3	5/3	5/3
1	1	12	F_{12}	1/3	5/3	5/3	5/3	1/3	5/3	1/3	5/3	1/3	5/3	1/3	5/3	5/3	5/3	1/3	5/3
1	1	13	F_{13}	1/3	5/3	5/3	5/3	5/3	1/3	1/3	1/3	5/3	5/3	5/3	1/3	5/3	5/3	5/3	1/3
1	1	2	F_2	1	1	1	1	1	1	1	1	1	1	1	1	1	1	1	1

TABLE II. Top: Indicates different types of intra- and interorbital scattering matrices and their properties under the discrete symmetries. The scattering matrices are labeled by $m = 0, \ldots, 15$ and appear as gamma matrices and their products. $\mathcal{T} = \mathcal{K}\gamma_1\gamma_3$, $\mathcal{I} = \gamma_0$, and $\mathcal{C} = \gamma_5$ correspond to time-reversal, inversion, and chiral symmetries, respectively. Bottom: The values of the dimensionless pair scattering rate $\tau_m \Gamma_{Jm} = 1 - 2b_{Jm}$ [where the matrix b_{Jm} is defined in Eq. (11)], which dictates how disorder affects superconductivity. It is clear that the F_{0g} state is protected from disorder that respects $\mathcal{T}$ symmetry (Anderson's theorem), while the F_{0u} state is protected from disorder that respects $\mathcal{CT}$ symmetry. In the last line, F_2 implies all the pairing states with $J = 2$, i.e., $F_{21} - F_{25}$. The result for all of these states is the same.

$$\tilde{g}_J = g_J/(1 + g_J \mathcal{P}_J), \tag{14}$$

where $\mathcal{P}_J = -T\sum_{\omega_n} \mathcal{B}_J(i\omega_n)$, and T is temperature. The transition temperature $T_{c,J}$ in the channel J is determined as a singularity (vanishing denominator) in Eq. (14), leading to the result that has the Abrikosov-Gor'kov form

$$\log\left(\frac{T_{c,J}}{T_{c,J,0}}\right) = \Psi(1/2) - \Psi\left(1/2 + \Gamma_J/4\pi T_{c,J}\right), \tag{15}$$

where $\Psi(x)$ is the digamma function, and $T_{c,J,0}$ is the transition temperature in the absence of any disorder. For the detailed calculation of the transition temperature, see Appendix C. An alternative derivation of this result via the method of Gor'kov Green's functions (which also gives a solution below T_c) is presented in Appendix D.

The solution of Eq. (15) predicts that superconductivity is completely suppressed at

$$\Gamma_{J\text{cr.}} = \pi e^{-\gamma_e} T_{c,J,0} \approx 1.76\, T_{c,J,0}, \tag{16}$$

($\gamma_e \approx 0.577...$ is the Euler's constant), as shown in Fig. 4.

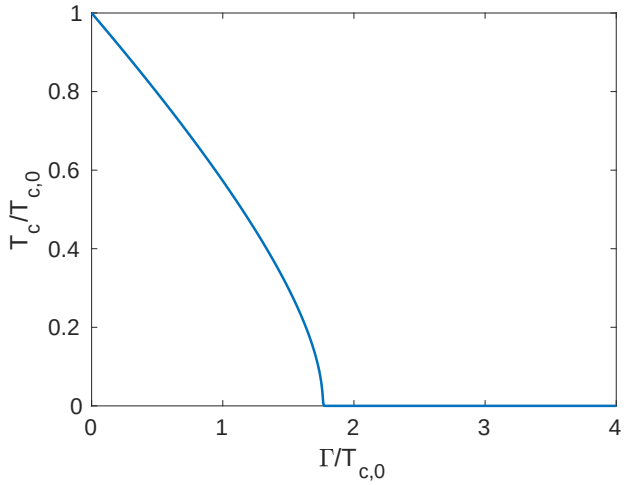

FIG. 4. $T_c/T_{c,0}$ as a function of $\Gamma/T_{c,0}$ obtained from the solution of Eq. (15).

IV. RESULTS

In Section III, we described how the pair scattering rates in Eq. (13) affect the transition temperature. As we show in Appendix D, the effect of these rates is actually much more general as they dictate the entire low-temperature thermodynamics of these superconductors (up to phase fluctuation effects) [2, 3]. For example, we recall that the gap may close in the superconducting state when disorder is sufficiently strong.

Having established the importance of the pair scattering rates in Eq. (13) for superconductivity in doped Dirac systems, we now turn to discuss their value for different pairing states and different interorbital disorder potentials. The results are summarized in Table II, which includes both non-magnetic ($m = 0, \ldots, 5$) and magnetic ($m = 6, \ldots, 15$) impurities.

As mentioned above, the elements of the matrix b_{Jm} in Eq. (11) range between $1/2$ and $-1/2$ (see Appendix B). Consequently, the rates Γ_{Jm} appearing in Table II, which shows the values of $1 - 2b_{Jm}$, range between 0 and twice the single particle scattering rate $1/\tau_m$. The former implies that disorder in channel m does not affect superconductivity in channel J, while the latter corresponds to the most severe effect possible.

Indeed, for the s-wave channel ($J = 0g$), we find that

the pair scattering rate vanishes, $\Gamma_{0g}=0$, for all the $\mathcal{T}$-even disorder matrices $m=0,\ldots,5$, which is manifestly the Anderson's theorem for non-magnetic impurities.

Additionally, we recover the well known Abrikosov-Gor'kov result for magnetic impurities, that the pair scattering rate is twice that of single particles [2], such that overall the pair-breaking rate is given by

$$\Gamma_{0g}=\sum_{m=6}^{15}\frac{2}{\tau_m}\,. \tag{17}$$

Another limit of interest is the odd-parity state with total angular momentum zero ($J=0u$), which is equivalent to the B-phase of superfluid ^{3}He [66]. We notice that, similar to the s-wave state F_{0g}, this pairing state is completely protected from certain types disorder, namely $m=0,2$ and $12,\ldots,15$. Inspecting Table II we identify that the common symmetry of these disorder potentials is that they are all even under the product of chiral and time reversal $\mathcal{CT}$. What makes this result even more interesting is that some of the $\mathcal{CT}$-even matrices are $\mathcal{T}$-odd. Thus, the F_{0u} is protected from certain types of magnetic impurities. We identify this protection with similar results for superconductors with multiple Fermi surfaces [52].

To understand this protection we now show that the F_{0u} is essentially a singlet pairing state between partners related to each other by $\mathcal{CT}$. Thus, in complete equivalence to the Anderson's original argument [1], it follows that as long as the disorder potential does not violate $\mathcal{CT}$ symmetry, we can always pair $\mathcal{CT}$ partners in the basis that diagonalizes the disorder potential.

Let us show that the F_{0u} pairing state is indeed a singlet state built out of $\mathcal{CT}$ partners. This is most easily seen in the orbital basis. We find it convenient to rotate the orbital basis by $\pi/2$ about the τ_2 axis first. This transforms from the basis of chirality to the basis of parity (i. e., the orbitals are labeled by their parity $\tau=\pm$). Note that this does not affect the operation of time-reversal $\mathcal{T}$. Then the action of chiral symmetry is implemented by $\mathcal{C}=\tilde{\gamma}_5=\tau_1 s_0$ and the corresponding pairing state F_{0u} is

$$\Delta_{0u}=\frac{1}{2}\psi_{\boldsymbol{k}}\mathcal{T}\tilde{\gamma}_5\psi_{\boldsymbol{k}}=\frac{1}{2}\left[\psi_{\downarrow+}(\boldsymbol{k})\psi_{\uparrow-}(-\boldsymbol{k})-\psi_{\uparrow+}(\boldsymbol{k})\psi_{\downarrow-}(-\boldsymbol{k})-\psi_{\uparrow-}(\boldsymbol{k})\psi_{\downarrow+}(-\boldsymbol{k})+\psi_{\downarrow-}(\boldsymbol{k})\psi_{\uparrow+}(-\boldsymbol{k})\right] \tag{18}$$

where $\psi_{s\tau}(\boldsymbol{k})$ is a field operator in the rotated basis. After inspecting this pairing state, it is evident that it is fully antisymmetric and that each term consists of a pair of operators related to each other by $\mathcal{CT}$ symmetry.

However, the F_{0u} state becomes vulnerable to disorder when $\mathcal{CT}$ symmetry is not present, such as in doped Bi_2Se_3. In that case mass belongs to the same representation as density and is always present. Moreover, we argue that Dirac materials are often polar ionic crystals (e.g. Bi_2Se_3, SnTe, PdTe etc.), therefore, it is likely that the disorder potential also induces dipolar moments of type $m=3,4,5$. This argument should be contrasted with the claim made in Ref. [67], where it was stated that only density disorder should be present. Overall, we find that the pair-breaking rate in the F_{0u} channel equals

$$\Gamma_{0u}=\frac{2}{\tau_1}+\sum_{m=3}^{11}\frac{2}{\tau_m}. \tag{19}$$

It should also be noted that the authors of Ref. [48] were the first ones to identify that the F_{0u} state can be protected from disorder in the massless limit. However, they concluded that it is protected by $\mathcal{C}$ symmetry. As we show here, it is actually protected by $\mathcal{CT}$ symmetry. To emphasize this distinction between the two, we point out that the F_{0u} state is immune to some disorder potentials that are odd under $\mathcal{C}$, such as $m=12,\ldots,15$.

Next, we consider the odd-parity pairing states with total angular momentum $J=1$. These states (more accurately, the nematic E_u states of the D_{3d} symmetry group of Bi_2Se_3, which derive from the $J=1$ representation by breaking the rotational symmetry from spherical to trigonal) are of special interest experimentally, since they are considered to be the pairing state in doped Bi_2Se_3 [28–35, 39, 49]. We find that all disorder channels affect superconductivity with this pairing symmetry, and the dimensionless rate $\tau_m\Gamma_m$ takes two possible values 5/3 and 1/3. Thus, depending on the relative weight in these channels, the scattering rate can vary significantly. In particular, for density disorder, the rate $\Gamma_{1j,0}=1/3\tau_0$ is much smaller than in systems without spin-orbit coupling, where it is expected to be $1/\tau_0$ [5, 11]. This is consistent with the findings of Refs. [46, 50, 51]. However, the $m>0$ channels are actually more harmful. For example, if polar disorder is present, then an average over all possible directions gives $\Gamma_{1j,3-5}=11/9\tau_3$, where we assume $\tau_3=\tau_4=\tau_5$ by symmetry.

V. DISCUSSION

In this paper, we construct a rigorous method to evaluate the effect of both intra- and interorbital disorder on superconductivity in doped Dirac materials. We argue that generic disorder potential always induces interorbital scattering processes given by Eq. (2) and listed in Table I. We compute the contribution of each type of

intra- and interorbital scattering channels to the pair-breaking rate for a given pairing potential, which dictates the entire thermodynamics of a superconductor. This result is summarized in Table II. Our main conclusions from this analysis are as follows:

- We have found a version of the Anderson's theorem which is based on the pairing of $\mathcal{CT}$-partners rather than $\mathcal{T}$-partners ($\mathcal{C}$ is chiral and $\mathcal{T}$ is time-reversal symmetry). The odd-parity state with total angular momentum zero ($J = 0u$) is such a pairing state. Consequently, it is protected from disorder that respects $\mathcal{CT}$ symmetry, which includes certain types of $\mathcal{T}$-odd impurities. This also generalizes the results of Ref. [48]. It is interesting to understand in the future if such a symmetry can exist (or nearly exist) in a solid state material.

- As expected from the Anderson's theorem, the s-wave ($J = 0g$) pairing state is protected from all non-magnetic scattering processes, including interorbital ones.

- The $J = 1$ states, which can be considered as the $O(3)$ analog of the multicomponent nematic candidate state for doped Bi_2Se_3 [28–35, 39, 49], can be weakly affected by disorder, depending on the specific details of the impurity potential. By "weakly" we mean significantly weaker than Larkin's result for p-wave superconductivity in systems without spin-orbit coupling [5].

We emphasize that the results obtained in this paper are based on a model where the mass term in the single-particle Hamiltonian, Eq. (1), was assumed to be zero. It should be noted, however, that in the majority of doped topological materials which become superconducting, such a mass term exists. We neglected it because of two reasons. The first one is that, in most cases, the Fermi energy is much larger than the mass (band gap). The second one is that the omission of the mass term allows us to obtain universal values for the scattering rates, as appears in Table II. As shown in Ref. [48], the inclusion of this term would modify these numbers towards their known values without spin-orbit coupling [2, 5]. In particular, it will remove the protection of the F_{0u} state.

The analysis performed in this work assumes a short-ranged disorder potential. However, in doped materials, one may also anticipate a correlated potential emerging from charged impurities [68]. Therefore, it is important to also understand the influence of a soft potential on superconductivity.

Another question which was not addressed in this paper is the microscopic origin of pairing and how it is affected by disorder [69]. In particular, doped topological materials are characterized by small electronic density and small density of states. As a result, the pairing interaction must be more singular [64]. Such an interaction is expected to be sensitive to the presence of disorder [70].

Finally, our results hold only for the case of a finite Fermi energy and weak disorder, implying $\epsilon_F \gg \Delta$ and $\epsilon_F \tau \gg 1$. It would be interesting to consider the limit of low density, where both conduction and valence bands are important. However, the methods used in this work are not powerful enough to deal with that limit [71].

Looking forward, we argue that our theory is useful to many other systems with strong orbital hybridization. In particular, Eq. (11) is easily generalizable to different Hamiltonians and reduced dimensions. Of special interest are semimetallic systems, including a quadratic band touching point relevant to the half-Heusler compounds [72], line-node semimetals, Weyl semimetals that emerge when inversion is broken in a Dirac material [64], and higher-order band touching points [73].

Before concluding this paper we note that arguments for robustness of unconventional superconductivity were recently casted in terms of the so-called "superconducting fitness" function [74]. As shown in Ref. [75], one can assess if disorder affects superconductivity by looking at the minimal excitation of a system and comparing it with the clean limit. When TRS is present, this is translated into the condition that the full Hamiltonian including disorder commutes with the gap function, $[\hat{H} + \hat{V}, \hat{\Delta}] = 0$ [47]. Our results are consistent with this picture. However, when the commutation relation is non-zero, as in some of the cases considered in this paper, it is not always straightforward to see the effect of disorder on the various pairing states based on the superconducting fitness. In particular, it is not clear to us how, using the fitness approach, to predict the protection of the F_{0u} state by $\mathcal{CT}$ symmetry or to obtain the significantly reduced pair-breaking rate in the F_{1j} states for certain types of disorder.

VI. ACKNOWLEDGMENTS

We are grateful to Rafael Fernandes, David Möckli, Maxim Khodas and Yuki Nagai for helpful discussions. JR and DD acknowledge the support of the Israeli Science Foundation under grant No. 967/19. VK was supported by the Quantum Materials program at LBNL, funded by the US Department of Energy under Contract No. DE-AC02-05CH11231.

Appendix A: Comparison with a parabolic dispersion: computation of Γ

Here we show the derivation of the Anderson's theorem for the case of a metal with parabolic dispersion without spin-orbit coupling. We use the method described in the main text. We start with the normal-state action for a clean metal:

$$\mathcal{S}_0 = \sum_{\omega,\boldsymbol{k}} \psi^\dagger_{\omega,\boldsymbol{k}} \left[-i\omega + \boldsymbol{k}^2/2m - \epsilon_F\right] \psi_{\omega,\boldsymbol{k}}, \tag{A1}$$

where the notations are the same as in the main text. We only consider density disorder in this Appendix, which corresponds to the $m = 0$ term in Eq. (2). As for the pairing potential, we focus on the s-wave channel, which is given by $F_J = F_{0g}$ in Eq. (4).

Single-particle lifetime – The self-energy within the first Born approximation (after linearizing near the Fermi energy) is given by

$$\Sigma(i\omega) = \frac{n_i V^2 k_F^2}{2\pi^2} \int_{-\infty}^{\infty} \frac{dk}{i\omega - v_F k} = -i\frac{\text{sign}(\omega)}{2\tau}. \quad \text{(A2)}$$

Here V^2 is the variance of the disorder potential V_l which has zero mean, $\tau^{-1} = (2\pi V^2 n_i \nu_0)$ is the scattering time, $\nu_0 = k_F^2/2\pi^2 v_F = m k_F/2\pi^2$ is the density of states (DOS) at the Fermi level per one spin, and $n_i = N_i/L^3$ is the total density of impurities. The resulting Green's function is then given by

$$G_{s,s'}(i\omega, \mathbf{k}) = \frac{\delta_{s,s'}}{i[\omega + \text{sign}(\omega)/2\tau] - \epsilon_{\mathbf{k}}}, \quad \text{(A3)}$$

where s, s' are the spin indices.

Vertex correction – Using the definition of the bare propagator of a Cooper pair, Eq. (9), we obtain

$$A(i\omega) = \frac{2\pi\tau\nu_0}{1 + 2\tau|\omega|}. \quad \text{(A4)}$$

L	S	J	$\mathcal{I}$	Basis function
0	0	0	+	$F_{0g} = \sqrt{\frac{1}{2}}(-i\sigma^y)$
1	1	0	-	$F_{0u} = \sqrt{\frac{1}{2}}(-i\sigma^y[\hat{\boldsymbol{k}} \cdot \boldsymbol{\sigma}])$
1	1	1	-	$F_{11} = \sqrt{\frac{3}{4}}(-i\sigma^y[-\hat{k}_z\sigma^y + \hat{k}^y\sigma^z])$
				$F_{12} = \sqrt{\frac{3}{4}}(-i\sigma^y[\hat{k}_z\sigma^x - \hat{k}^x\sigma^z])$
				$F_{13} = \sqrt{\frac{3}{4}}(-i\sigma^y[-\hat{k}_y\sigma^x + \hat{k}^x\sigma^y])$
1	1	2	-	$F_{21} = \sqrt{\frac{3}{4}}(-i\sigma^y[\hat{k}_x\sigma^y + \hat{k}^y\sigma^x])$
				$F_{22} = \sqrt{\frac{3}{4}}(-i\sigma^y[\hat{k}_y\sigma^z + \hat{k}^z\sigma^y])$
				$F_{23} = \sqrt{\frac{3}{4}}(-i\sigma^y[\hat{k}_x\sigma^z + \hat{k}^z\sigma^x])$
				$F_{24} = \sqrt{\frac{3}{4}}(-i\sigma^y[\hat{k}_x\sigma^x - \hat{k}^y\sigma^y])$
				$F_{25} = \sqrt{\frac{1}{4}}(-i\sigma^y[-\hat{k}_x\sigma^x - \hat{k}^y\sigma^y + 2\hat{k}_z\sigma^z])$

TABLE III. Different representations of the time-reversal-invariant order parameters F_J. Note that for every total angular momentum J there are $2J + 1$ states $|J, J_z\rangle$, where J_z gets integer values between $-J$ and J. Thus, the two different states with $J = 0$ both have $J_z = 0$ and are distinguished by their transformation properties under inversion, either even (g) or odd (u).

The ladder summation of Eq. (A4) with the non-crossing impurity lines (Cooperon) gives

$$\mathcal{B}_J(i\omega) = \frac{A(i\omega)}{1 - V^2 n_i A(i\omega)} = \frac{\pi\nu_0}{|\omega|}. \quad \text{(A5)}$$

Computation of T_c – Finally, we perform the summation over Matsubara frequencies $\omega_n = \pi T(2n + 1)$ and find

$$\mathcal{P} = -T\sum_{\omega_n} \mathcal{B}_J(i\omega_n) = -\nu_0 \log \omega_D/T_c, \quad \text{(A6)}$$

where ω_D is the cut-off Debye frequency. Consequently, the effective interaction constant is given by

$$\tilde{g} = \frac{g}{1 + g\mathcal{P}}, \quad \text{(A7)}$$

and the instability occurs at $g\mathcal{P} + 1 = 0$. The critical temperature then equals

$$T_c = \omega_D e^{-1/g\nu_0}, \quad \text{(A8)}$$

which is the well-known BCS result. We see that density disorder does not modify the transition temperature for the s-wave pairing, which is exactly the statement of the Anderson's theorem [1]. As we also show below in Appendix D, non-magnetic disorder does not change the whole thermodynamics of the s-wave superconductors [3].

Appendix B: Table of the basis functions $F_J(\hat{\boldsymbol{k}})$ and the conversion matrix b_{Jm}

In Eq. (4) of the main text, we assumed that the attractive interaction is already projected onto the Fermi surface and decomposed into different pairing channels, which correspond to the representations of the point group symmetry. For simplicity, in this paper we focus on the $O(3)$ symmetry group of joint rotations of momentum and spin. Different superconducting channels are characterized then by total angular momentum J, while spin S and orbital L angular momenta are not good quantum numbers because of strong spin-orbit coupling. The basis functions $F_J(\hat{\boldsymbol{k}})$ corresponding to different channels up to order $J = 2$ (and $L = 1$) were obtained in Refs. [40, 49, 63] and are listed in Table III.

Finally, the matrix elements b_{Jm} from Eq. (11), where $m = 0 - 15$ numerates different types of disorder, equal to

$$b_{Jm} = \begin{pmatrix} 1/2 & 1/2 & 1/2 & 1/2 & 1/2 & 1/2 & -1/2 & -1/2 & -1/2 & -1/2 & -1/2 & -1/2 & -1/2 & -1/2 & -1/2 & -1/2 \\ 1/2 & -1/2 & 1/2 & -1/2 & -1/2 & -1/2 & -1/2 & -1/2 & -1/2 & -1/2 & -1/2 & -1/2 & 1/2 & 1/2 & 1/2 & 1/2 \\ 1/3 & -1/3 & -1/3 & 1/3 & -1/3 & -1/3 & -1/3 & 1/3 & 1/3 & 1/3 & -1/3 & -1/3 & -1/3 & 1/3 & -1/3 & -1/3 \\ 1/3 & -1/3 & -1/3 & -1/3 & 1/3 & -1/3 & 1/3 & -1/3 & 1/3 & -1/3 & 1/3 & -1/3 & -1/3 & -1/3 & 1/3 & -1/3 \\ 1/3 & -1/3 & -1/3 & -1/3 & -1/3 & 1/3 & 1/3 & 1/3 & -1/3 & -1/3 & -1/3 & 1/3 & -1/3 & -1/3 & -1/3 & 1/3 \\ 0 & 0 & 0 & 0 & 0 & 0 & 0 & 0 & 0 & 0 & 0 & 0 & 0 & 0 & 0 & 0 \end{pmatrix}. \tag{B1}$$

The last line of this matrix describes *all* channels with $J = 2$ [i.e., $F_{21}(\hat{\boldsymbol{k}}) - F_{25}(\hat{\boldsymbol{k}})$].

Appendix C: Calculation of T_c

Using the condition for the superconducting instability, Eq. (14) of the main text, we obtain that $\mathcal{P} \equiv -T_c \sum_\omega \mathcal{B}(i\omega) = -\frac{1}{g}$. Note that the derivation in this Appendix is independent of the pairing channel, so we omit the subscript J for brevity. We now plug in the result for $\mathcal{B}(i\omega)$ as obtained in Eq. (12) and find

$$\frac{1}{g} = T_c \sum_n \frac{\pi\nu_0}{\Gamma/2 + |\omega_n|}. \tag{C1}$$

Using the definition of Matsubara frequencies $\omega_n = 2\pi T(n + 1/2)$, this equation can be rewritten as

$$\frac{2}{g\nu_0} = \sum_n \frac{1}{\Gamma/4\pi T_c + |n + 1/2|}. \tag{C2}$$

Following Abrikosov and Gor'kov [2], we make use of the fact that in the clean limit one has

$$\sum_{n\geq 0} \frac{1}{n + 1/2} = \log\left(\frac{4e^{\gamma_e}}{\pi}\frac{\omega_D}{2T_c}\right), \tag{C3}$$

where γ_e is the Euler's constant. Thus, we can rewrite Eq. (C2) as

$$\begin{aligned} \frac{1}{g\nu_0} &= \sum_{n\geq 0} \frac{1}{\Gamma/4\pi T_c + (n + 1/2)} = \sum_{n\geq 0}\left[\frac{1}{\Gamma/4\pi T_c + (n + 1/2)} - \frac{1}{n + 1/2}\right] + \log\left(\frac{4e^{\gamma_e}}{\pi}\frac{\omega_D}{2T_c}\right) \\ &= \sum_{n\geq 0}\left[\frac{1}{(n + 1/2 + \Gamma/4\pi T_c)} - \frac{1}{(n+1)} + \frac{1}{(n+1)} - \frac{1}{(n+1/2)}\right] + \log\left(\frac{4e^{\gamma_e}}{\pi}\frac{\omega_D}{2T_c}\right). \end{aligned} \tag{C4}$$

We can identify the two terms inside the square brackets as digamma function

$$\Psi(z) = -\gamma_e + \sum_{n\geq 0}\left[\frac{1}{(n+1)} - \frac{1}{(n+z)}\right], \tag{C5}$$

and we know from Eq. (C3) that $\frac{1}{g\nu_0} = \log\left(\frac{4e^{\gamma_e}}{\pi}\frac{\omega_D}{2T_{c,0}}\right)$, where $T_{c,0}$ is the critical temperature for a clean system. Consequently, we obtain

$$\begin{aligned} \log\left(\frac{4e^{\gamma_e}}{\pi}\frac{\omega_D}{2T_{c,0}}\right) = \Psi(1/2) - \Psi(1/2 + \Gamma/4\pi T_c) + \\ + \log\left(\frac{4e^{\gamma_e}}{\pi}\frac{\omega_D}{2T_c}\right), \end{aligned} \tag{C6}$$

or

$$\log\left(\frac{T_c}{T_{c,0}}\right) = \Psi(1/2) - \Psi(1/2 + \Gamma/4\pi T_c), \tag{C7}$$

which coincides with Eq. (15) of the main text.

Appendix D: Abrikosov-Gor'kov equations at arbitrary temperature: gapless superconductivity.

Now we present the complementary approach to derive the effect of disorder on superconductivity, which exploits the formalism of Gor'kov Green's functions [76]. The advantage of this method is that it allows to treat the problem at arbitrary temperature and study thermodynamic and electromagnetic properties of a disordered superconductor at temperatures down to $T = 0$.

To start with, we introduce the Nambu space (N) for the MCBB electron operators according to

$$\Psi_{\boldsymbol{k}} = \begin{pmatrix} c_{\boldsymbol{k},1} \\ c_{\boldsymbol{k},2} \\ c^\dagger_{-\boldsymbol{k},1} \\ c^\dagger_{-\boldsymbol{k},2} \end{pmatrix}_N. \tag{D1}$$

In this basis, the bare (without disorder) Gor'kov Green's function takes form [65, 77]

$$\hat{G}_0(i\omega_n,\boldsymbol{k}) = -\frac{i\omega_n\hat{\tau}_0 + \xi_{\boldsymbol{k}}\hat{\tau}_3 + \hat{\Delta}_{\boldsymbol{k}}}{\omega_n^2+\xi_{\boldsymbol{k}}^2+\Delta_{\boldsymbol{k}}^2}, \tag{D2}$$

where

$$\hat{\Delta}_{\boldsymbol{k}} = \sqrt{2}\Delta \begin{pmatrix} 0 & F^\dagger(\hat{\boldsymbol{k}}) \\ F(\hat{\boldsymbol{k}}) & 0 \end{pmatrix}_N, \tag{D3}$$

and

$$\Delta_{\boldsymbol{k}}^2 \equiv \Delta^2 \mathrm{Tr}\, F^\dagger(\hat{\boldsymbol{k}})F(\hat{\boldsymbol{k}}). \tag{D4}$$

Matrices $\hat{\tau}_0$ and $\hat{\tau}_3$ here are the corresponding Pauli matrices in the Nambu space (not to be confused with the Pauli matrices in the orbital basis). The factor $\sqrt{2}$ in Eq. (D3) is introduced for convenience only, and simply reflects the normalization condition for functions $F(\hat{\boldsymbol{k}})$. The form of the Gor'kov Green's function (D2) holds for the states with unitary pairing, i.e., satisfying the relation $\hat{\Delta}_{\boldsymbol{k}}^\dagger\hat{\Delta}_{\boldsymbol{k}} \propto \mathbb{1}$. The non-unitary states [77], which do not satisfy this relation and can be realized in multi-component superconductors, will be considered in future works.

The matrices $Q_m^{\alpha\beta}(\boldsymbol{p},\boldsymbol{k}) \equiv \langle\hat{\boldsymbol{p}}\alpha|M_m|\hat{\boldsymbol{k}}\beta\rangle$, describing the scattering of electrons on the impurities of type m in the MCBB basis, in the Nambu space become

$$Q_m(\hat{\boldsymbol{p}},\hat{\boldsymbol{k}}) \to \hat{Q}_m(\hat{\boldsymbol{p}},\hat{\boldsymbol{k}}) = \begin{pmatrix} Q_m(\hat{\boldsymbol{p}},\hat{\boldsymbol{k}}) & 0 \\ 0 & -Q_m^T(-\hat{\boldsymbol{k}},-\hat{\boldsymbol{p}}) \end{pmatrix}_N. \tag{D5}$$

The self-energy due to disorder is then given by

$$\hat{\Sigma}_m(i\omega_n,\hat{\boldsymbol{p}}) = n_m V_m^2 \int \frac{d^3k}{(2\pi)^3}\hat{Q}_m(\hat{\boldsymbol{p}},\hat{\boldsymbol{k}})\hat{G}(i\omega_n,\boldsymbol{k})\hat{Q}_m(\hat{\boldsymbol{k}},\hat{\boldsymbol{p}}). \tag{D6}$$

We notice that the self-consistency requires us to use full Green's function $\hat{G}$, instead of the bare one $\hat{G}_0$. Following Ref. [2], we look for a solution of the form

$$\hat{G}(i\omega_n,\boldsymbol{k}) = -\frac{i\tilde{\omega}_n\hat{\tau}_0 + \xi_{\boldsymbol{k}}\hat{\tau}_3 + \tilde{\Delta}_{n,\boldsymbol{k}}}{\tilde{\omega}_n^2+\xi_{\boldsymbol{k}}^2+\tilde{\Delta}_{n,\boldsymbol{k}}^2}, \tag{D7}$$

with

$$\tilde{\Delta}_{n,\boldsymbol{k}} = \sqrt{2}\tilde{\Delta}_n \begin{pmatrix} 0 & F^\dagger(\hat{\boldsymbol{k}}) \\ F(\hat{\boldsymbol{k}}) & 0 \end{pmatrix}_N, \tag{D8}$$

and

$$\tilde{\Delta}_{n,\boldsymbol{k}}^2 \equiv \tilde{\Delta}_n^2 \mathrm{Tr}\, F^\dagger(\hat{\boldsymbol{k}})F(\hat{\boldsymbol{k}}). \tag{D9}$$

Performing integration over $\xi_{\boldsymbol{k}}$ first, we obtain the very general expression which applies to any superconducting state with unitary pairing:

$$\hat{\Sigma}_m(i\omega_n,\hat{\boldsymbol{p}}) = -n_m V_m^2 \pi\nu_0 \int \frac{d\Omega_{\boldsymbol{k}}}{4\pi}\hat{Q}_m(\hat{\boldsymbol{p}},\hat{\boldsymbol{k}})\times \\ \times \frac{i\tilde{\omega}_n\hat{\tau}_0 + \tilde{\Delta}_{n,\boldsymbol{k}}}{\sqrt{\tilde{\omega}_n^2+\tilde{\Delta}_{n,\boldsymbol{k}}^2}}\hat{Q}_m(\hat{\boldsymbol{k}},\hat{\boldsymbol{p}}). \tag{D10}$$

The above expression can be easily used to reproduce the result for the transition temperature $T_{c,J}$, Eq. (15). Neglecting $\tilde{\Delta}_{n,\boldsymbol{k}}^2$ in the denominator and performing integration over $\hat{\Omega}_{\boldsymbol{k}}$ and summation over m, we find for the channel J

$$\hat{\Sigma}(i\omega_n,\hat{\boldsymbol{p}}) \equiv \sum_m \hat{\Sigma}_m(i\omega_n,\hat{\boldsymbol{p}}) = \\ = -\frac{i\hat{\tau}_0\mathrm{sign}(\tilde{\omega}_n)}{2\tau} + \frac{\tilde{\Delta}_{n,\boldsymbol{p}}(1-\tau\Gamma_J)}{2\tau|\tilde{\omega}_n|}, \tag{D11}$$

where Γ_J is given by Eq. (13). In deriving the last equation, we also used Eqs. (10) and (11). Utilizing further Dyson equation $\hat{G}^{-1} = \hat{G}_0^{-1} - \hat{\Sigma}$, we easily obtain

$$\tilde{\omega}_n = \omega_n + \frac{\mathrm{sign}(\tilde{\omega}_n)}{2\tau}, \\ \tilde{\Delta}_n = \Delta + \frac{\tilde{\Delta}_n(1-\tau\Gamma_J)}{2\tau|\tilde{\omega}_n|}, \tag{D12}$$

which can be readily resolved yielding

$$\tilde{\omega}_n = \omega_n + \frac{\mathrm{sign}(\omega_n)}{2\tau}, \\ \tilde{\Delta}_n = \Delta\left(1 - \frac{1-\tau\Gamma_J}{2\tau|\tilde{\omega}_n|}\right)^{-1}. \tag{D13}$$

Finally, using the gap equation in the channel J

$$\hat{\Delta}_{\boldsymbol{k},\alpha\beta} = g_J T_c \sum_{n,\boldsymbol{p}} F^\dagger_{J\alpha\beta}(\hat{\boldsymbol{k}})F_{J\gamma\delta}(\hat{\boldsymbol{p}})\frac{\tilde{\Delta}_{n,\boldsymbol{p},\delta\gamma}}{\tilde{\omega}_n^2+\xi_{\boldsymbol{p}}^2}, \tag{D14}$$

we obtain after summation over $\boldsymbol{p}$

$$1 = \pi g_J T_c \nu_0 \sum_n \frac{1}{\Gamma_J/2 + |\tilde{\omega}_n| - \frac{1}{2\tau}} = \\ = \pi g_J T_c \nu_0 \sum_n \frac{1}{\Gamma_J/2 + |\omega_n|}, \tag{D15}$$

which is identical to Eq. (C1) and leads eventually to Eq. (15).

We emphasize that Eq. (D10) is very general and can be used to study thermodynamic properties of any (unitary) superconducting state. As an example, we focus on the fully isotropic pairing functions F_{0g} and F_{0u}. Performing integration over $\Omega_{\boldsymbol{k}}$ in Eq. (D10), we find a set of coupled equations for $\tilde{\omega}_n$ and $\tilde{\Delta}_n$:

$$\tilde{\omega}_n = \omega_n + \frac{\tilde{\omega}_n}{2\tau\sqrt{\tilde{\omega}_n^2 + \tilde{\Delta}_n^2}},$$
$$\tilde{\Delta}_n = \Delta + \frac{\tilde{\Delta}_n(1-\tau\Gamma_J)}{2\tau\sqrt{\tilde{\omega}_n^2 + \tilde{\Delta}_n^2}}, \tag{D16}$$

accompanied with the gap equation

$$\Delta = \pi g_J T \nu_0 \sum_n \frac{\tilde{\Delta}_n}{\sqrt{\tilde{\omega}_n^2 + \tilde{\Delta}_n^2}}. \tag{D17}$$

These equations, in principle, can be solved numerically to find the value of the pairing gap Δ at arbitrary temperature and study the thermodynamic properties of a superconductor. For instance, in the case of non-magnetic ($\mathcal{T}$-even) disorder for the s-wave F_{0g} pairing or $\mathcal{CT}$-even disorder for the p-wave F_{0u} pairing, we have $\Gamma_J = 0$, and Eq. (D16) admits simple solution $\tilde{\omega}_n/\tilde{\Delta}_n = \omega_n/\Delta$. In these cases, the latter result implies that the gap equation (D17) is not modified by disorder at all, consequently, the transition temperature and all the thermodynamic properties below T_c remain unchanged compared to the clean case.

Abrikosov and Gor'kov have analyzed Eqs. (D16) and (D17) in detail (with $\Gamma_J \neq 0$) for the most interesting limiting cases in Ref. [2]. In particular, they found that there is a range of the impurity concentration where superconductivity is not entirely suppressed, while becoming gapless. In our language, this corresponds to the threshold value of the pair-breaking rate Γ'_J, above which the gap in the spectrum of elementary excitations vanishes:

$$\Gamma'_J = 2e^{-\pi/4}\Gamma_{J\text{cr.}} \approx 0.91\,\Gamma_{J\text{cr.}}, \tag{D18}$$

where the critical value $\Gamma_{J\text{cr.}}$ is given by Eq. (16). As a result, the low-temperature behavior of the specific heat changes from exponential to T-linear in the range $\Gamma'_J < \Gamma_J < \Gamma_{J\text{cr.}}$.

The analysis of this Appendix can be straightforwardly generalized to study the effect of different types of disorder on the anisotropic nematic pairing states in doped Bi_2Se_3 compounds [39, 49] or non-unitary chiral pairing in Majorana superconductors [49, 78]. We leave these and related interesting questions to a future publication.

[1] P. Anderson, Journal of Physics and Chemistry of Solids **11**, 26 (1959).
[2] A. A. Abrikosov and L. P. Gor'kov, Zh. Eksp. Teor. Fiz. **39**, 1781 (1960).
[3] L. P. Gor'kov, "Theory of superconducting alloys," in *Superconductivity: Conventional and Unconventional Superconductors*, edited by K. H. Bennemann and J. B. Ketterson (Springer Berlin Heidelberg, Berlin, Heidelberg, 2008) pp. 201–224.
[4] M. Ma and P. A. Lee, Phys. Rev. B **32**, 5658 (1985).
[5] A. I. Larkin, Pis'ma Zh. Eksp. Teor. Fiz. **2**, 205 (1965).
[6] A. J. Millis, S. Sachdev, and C. M. Varma, Phys. Rev. B **37**, 4975 (1988).
[7] R. J. Radtke, K. Levin, H.-B. Schüttler, and M. R. Norman, Phys. Rev. B **48**, 653 (1993).
[8] P. J. Hirschfeld and N. Goldenfeld, Phys. Rev. B **48**, 4219 (1993).
[9] V. Emery and S. Kivelson, Nature **374**, 434 (1995).
[10] Y. Dalichaouch, M. C. de Andrade, D. A. Gajewski, R. Chau, P. Visani, and M. B. Maple, Phys. Rev. Lett. **75**, 3938 (1995).
[11] A. P. Mackenzie, R. K. W. Haselwimmer, A. W. Tyler, G. G. Lonzarich, Y. Mori, S. Nishizaki, and Y. Maeno, Phys. Rev. Lett. **80**, 161 (1998).
[12] A. P. Mackenzie and Y. Maeno, Rev. Mod. Phys. **75**, 657 (2003).
[13] K. Fujita, T. Noda, K. M. Kojima, H. Eisaki, and S. Uchida, Phys. Rev. Lett. **95**, 097006 (2005).
[14] S. Florens and M. Vojta, Phys. Rev. B **71**, 094516 (2005).
[15] H. Alloul, J. Bobroff, M. Gabay, and P. Hirschfeld, Reviews of Modern Physics **81**, 45 (2009).
[16] C. Tarantini, M. Putti, A. Gurevich, Y. Shen, R. K. Singh, J. M. Rowell, N. Newman, D. C. Larbalestier, P. Cheng, Y. Jia, and H.-H. Wen, Phys. Rev. Lett. **104**, 087002 (2010).
[17] J. Li, Y. F. Guo, S. B. Zhang, J. Yuan, Y. Tsujimoto, X. Wang, C. I. Sathish, Y. Sun, S. Yu, W. Yi, K. Yamaura, E. Takayama-Muromachiu, Y. Shirako, M. Akaogi, and H. Kontani, Phys. Rev. B **85**, 214509 (2012).
[18] K. Kirshenbaum, S. R. Saha, S. Ziemak, T. Drye, and J. Paglione, Phys. Rev. B **86**, 140505 (2012).
[19] Y. Mizukami, M. Konczykowski, Y. Kawamoto, S. Kurata, S. Kasahara, K. Hashimoto, V. Mishra, A. Kreisel, Y. Wang, P. Hirschfeld, *et al.*, Nature communications **5**, 1 (2014).
[20] I. Božović, X. He, J. Wu, and A. Bollinger, Nature **536**, 309 (2016).
[21] N. Lee-Hone, J. Dodge, and D. Broun, Physical Review B **96**, 024501 (2017).
[22] E. Khestanova, J. Birkbeck, M. Zhu, Y. Cao, G. Yu, D. Ghazaryan, J. Yin, H. Berger, L. Forro, T. Taniguchi, *et al.*, Nano letters **18**, 2623 (2018).
[23] Y. S. Hor, A. J. Williams, J. G. Checkelsky, P. Roushan, J. Seo, Q. Xu, H. W. Zandbergen, A. Yazdani, N. P. Ong, and R. J. Cava, Physical review letters **104**, 057001 (2010).
[24] L. A. Wray, S.-Y. Xu, Y. Xia, Y. San Hor, D. Qian, A. V. Fedorov, H. Lin, A. Bansil, R. J. Cava, and M. Z. Hasan, Nature Physics **6**, 855 (2010).
[25] N. P. Butch, P. Syers, K. Kirshenbaum, A. P. Hope, and J. Paglione, Physical Review B **84**, 220504 (2011).

[26] S. Sasaki, Z. Ren, A. Taskin, K. Segawa, L. Fu, and Y. Ando, Physical review letters **109**, 217004 (2012).
[27] H. Wang, H. Wang, H. Liu, H. Lu, W. Yang, S. Jia, X.-J. Liu, X. Xie, J. Wei, and J. Wang, Nature materials **15**, 38 (2016).
[28] K. Matano, M. Kriener, K. Segawa, Y. Ando, and G.-q. Zheng, Nature Physics **12**, 852 (2016).
[29] S. Yonezawa, K. Tajiri, S. Nakata, Y. Nagai, Z. Wang, K. Segawa, Y. Ando, and Y. Maeno, Nature Physics **13**, 123 (2017).
[30] K. Willa, R. Willa, K. W. Song, G. D. Gu, J. A. Schneeloch, R. Zhong, A. E. Koshelev, W.-K. Kwok, and U. Welp, Phys. Rev. B **98**, 184509 (2018).
[31] Y. Pan, A. M. Nikitin, G. K. Araizi, Y. K. Huang, Y. Matsushita, T. Naka, and A. de Visser, Scientific Reports **6**, 28632 (2016).
[32] A. M. Nikitin, Y. Pan, Y. K. Huang, T. Naka, and A. de Visser, Phys. Rev. B **94**, 144516 (2016).
[33] T. Asaba, B. J. Lawson, C. Tinsman, L. Chen, P. Corbae, G. Li, Y. Qiu, Y. S. Hor, L. Fu, and L. Li, Phys. Rev. X **7**, 011009 (2017).
[34] R. Tao, Y.-J. Yan, X. Liu, Z.-W. Wang, Y. Ando, Q.-H. Wang, T. Zhang, and D.-L. Feng, Phys. Rev. X **8**, 041024 (2018).
[35] J. Shen, W.-Y. He, N. F. Q. Yuan, Z. Huang, C.-w. Cho, S. H. Lee, Y. San Hor, K. T. Law, and R. Lortz, npj Quantum Materials **2** (2017).
[36] H. Kim, K. Wang, Y. Nakajima, R. Hu, S. Ziemak, P. Syers, L. Wang, H. Hodovanets, J. D. Denlinger, P. M. Brydon, *et al.*, Science advances **4**, eaao4513 (2018).
[37] L. Fu and E. Berg, Phys. Rev. Lett. **105**, 097001 (2010).
[38] M. Sato, Phys. Rev. B **81**, 220504 (2010).
[39] L. Fu, Phys. Rev. B **90**, 100509 (2014).
[40] V. Kozii and L. Fu, Phys. Rev. Lett. **115**, 207002 (2015).
[41] P. Brydon, L. Wang, M. Weinert, and D. Agterberg, Physical review letters **116**, 177001 (2016).
[42] L. Savary, J. Ruhman, J. W. F. Venderbos, L. Fu, and P. A. Lee, Phys. Rev. B **96**, 214514 (2017).
[43] M. Kriener, K. Segawa, S. Sasaki, and Y. Ando, Physical Review B **86**, 180505 (2012).
[44] M. Novak, S. Sasaki, M. Kriener, K. Segawa, and Y. Ando, Physical Review B **88**, 140502 (2013).
[45] M. Smylie, K. Willa, H. Claus, A. Snezhko, I. Martin, W.-K. Kwok, Y. Qiu, Y. S. Hor, E. Bokari, P. Niraula, *et al.*, Physical Review B **96**, 115145 (2017).
[46] L. Andersen, A. Ramires, Z. Wang, T. Lorenz, and Y. Ando, Science Advances **6**, eaay6502 (2020).
[47] E. Timmons, S. Teknowijoyo, M. Kończykowski, O. Cavani, M. Tanatar, S. Ghimire, K. Cho, Y. Lee, L. Ke, N. H. Jo, *et al.*, arXiv:2001.04673 (2020).
[48] K. Michaeli and L. Fu, Physical review letters **109**, 187003 (2012).
[49] J. W. F. Venderbos, V. Kozii, and L. Fu, Phys. Rev. B **94**, 180504 (2016).
[50] Y. Nagai, Physical Review B **91**, 060502 (2015).
[51] D. Cavanagh and P. Brydon, Physical Review B **101**, 054509 (2020).
[52] A. A. Golubov and I. Mazin, Physical Review B **55**, 15146 (1997).
[53] J. Zhang, R. Sknepnek, R. M. Fernandes, and J. Schmalian, Physical Review B **79**, 220502 (2009).
[54] D. Efremov, M. Korshunov, O. Dolgov, A. A. Golubov, and P. Hirschfeld, Physical Review B **84**, 180512 (2011).
[55] Y. Wang, A. Kreisel, P. Hirschfeld, and V. Mishra, Physical Review B **87**, 094504 (2013).
[56] T. V. Trevisan, M. Schütt, and R. M. Fernandes, Physical Review B **98**, 094514 (2018).
[57] D. Möckli and M. Khodas, Physical Review B **98**, 144518 (2018).
[58] Y. Ando and L. Fu, Annu. Rev. Condens. Matter Phys. **6**, 361 (2015).
[59] N. F. Q. Yuan, W.-Y. He, and K. T. Law, Phys. Rev. B **95**, 201109 (2017).
[60] L. Chirolli, F. de Juan, and F. Guinea, Phys. Rev. B **95**, 201110 (2017).
[61] L. Chirolli, Phys. Rev. B **98**, 014505 (2018).
[62] L. Chirolli, arXiv:2002.07240 (2020).
[63] L. Fu, Physical review letters **115**, 026401 (2015).
[64] V. Kozii, Z. Bi, and J. Ruhman, Phys. Rev. X **9**, 031046 (2019).
[65] V. P. Mineev and K. V. Samokhin, *Introduction to Unconventional Superconductivity* (CRC Press, 1999).
[66] M. Salomaa and G. Volovik, EPL (Europhysics Letters) **2**, 781 (1986).
[67] L. Andersen, Z. Wang, T. Lorenz, and Y. Ando, Physical Review B **98**, 220512 (2018).
[68] B. Skinner, Phys. Rev. B **90**, 060202 (2014).
[69] A. Finkel'stein, Physica B: Condensed Matter **197**, 636 (1994).
[70] P. A. Lee and T. V. Ramakrishnan, Rev. Mod. Phys. **57**, 287 (1985).
[71] R. Nandkishore, J. Maciejko, D. A. Huse, and S. L. Sondhi, Physical Review B **87**, 174511 (2013).
[72] Y. Nakajima, R. Hu, K. Kirshenbaum, A. Hughes, P. Syers, X. Wang, K. Wang, R. Wang, S. R. Saha, D. Pratt, *et al.*, Science advances **1**, e1500242 (2015).
[73] B. Bradlyn, L. Elcoro, J. Cano, M. Vergniory, Z. Wang, C. Felser, M. Aroyo, and B. A. Bernevig, Nature **547**, 298 (2017).
[74] A. Ramires, D. F. Agterberg, and M. Sigrist, Physical Review B **98**, 024501 (2018).
[75] A. C. Potter and P. A. Lee, Physical Review B **83**, 184520 (2011).
[76] L. P. Gor'kov, Zh. Eksp. Teor. Fiz. **34**, 735 (1958).
[77] M. Sigrist and K. Ueda, Rev. Mod. Phys. **63**, 239 (1991).
[78] V. Kozii, J. W. F. Venderbos, and L. Fu, Science Advances **2** (2016).